JOURNAL OF MATERIALS SCIENCE 31 (1996) 5573–5582

Influence of reprocessing on properties of polycarbonate

A. CHRYSOSTOMOU, S. HASHEMI
School of Polymer Technology, University of North London, Holloway Road, London N7 8DB, UK

The influence of reprocessing by injection moulding on properties of polycarbonate has been studied. It was found that reprocessing does not affect the tensile strength, flexural strength and flexural modulus of the polycarbonate material. Fracture parameters such as fracture toughness and the material resistance to crack propagation, also showed no variation with the number of reprocessing cycles, although both were strongly dependent on sample width. Dynamic mechanical analysis (DMA) also indicated that reprocessing has no significant effect upon dynamic mechanical properties of polycarbonate. Results further indicated that the glass transition temperature of polycarbonate is not affected by reprocessing, only the range over which it occurs seems to be broadened by reprocessing due to increase in molecular weight with number of reprocessing cycles.

1. Introduction

In recent years the practice of recycling has been encouraged and promoted with the increased awareness in environmental matters and the subsequent desire to save resources. This together with the relatively high cost of the polymer and sometimes high levels of scrap material generated during manufacture, make this procedure both a viable and attractive option.

Several papers have been published concerning the effect of recycling on mechanical properties of polycarbonate [e.g. 1–2]. These studies have been mainly concerned with the effect of reprocessing on tensile properties and flow ability of polycarbonate. For example, studies by Abbas [1] and Eguiazabal and Nazabal [2] have shown that while reprocessing has no significant effect upon tensile strength, it influences the flow ability of these materials quite considerably. These studies have also indicated that a significant amount of chain session occurs during reprocessing and this leads to a material with a higher molecular weight and a lower impact strength. However, surprisingly, apart from studies by Chrysostomou and Hashemi on glass fibre reinforced polycarbonate [3], there is little, if any, information regarding the effect of reprocessing on fracture toughness and crack growth behaviour of reprocessed polycarbonate.

The main purpose of this paper is to study the influence of reprocessing not only on tensile properties of polycarbonate but also on flexural properties, dynamic mechanical properties, fracture toughness and crack growth resistance of this polymer.

2. Materials

The polycarbonate material used in this study was Makrolon 2805 obtained from Bayer UK. The material was dried in a conventional oven at 120 °C for a minimum of 4 h prior to processing.

3. Mouldings

Three types of specimens were injection moulded (see Fig. 1);

1 *Tensile bars* Dumbbell shaped specimens (see Fig. 1) of dimensions $1.7 \times 12.5 \times 125$ mm were produced on a Negri Bossi NB60 with a melt temperature of 300 °C and a mould temperature of 80 °C. Injection speed reached 208 r.p.m. while the pressure was held at 8 MPa. The mould used contained two cavities, a single feed and a double feed cavity in which the two opposing melt fronts meet to form a weldline mid-way along the gauge length.

2 *Flexural bars* Flexural specimens were produced on a Szekely Hydroject injection moulding machine using an edge-gated rectangular cavity of dimensions $4 \times 10 \times 120$ mm (see Fig. 1). The processing temperature was set at 290 °C and the mould temperature was set at 40 °C with a pressure of 3.79 MPa.

3 *Plaques* Square plaques of dimensions $88 \times 88 \times 1.5$ mm were produced on a Peco 15MR injection moulding machine. The mould cavity was filled by the molten material entering through a centrally positioned edge gate, as shown in Fig. 1. Plaques were processed at a melt temperature of 300 °C and a mould temperature of 80 °C with pressure attaining 10.35 MPa.

0022–2461

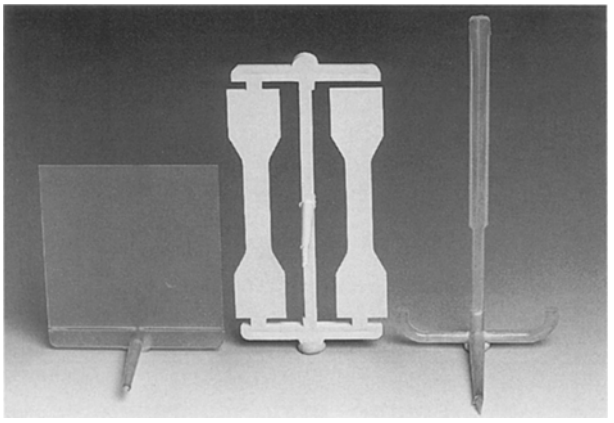

Figure 1 Injection mouldings used: tensile bars, flexural bars and plaque mouldings.

4. Reprocessing

The material that was supplied by the manufacturer was first injection moulded into the test specimens. On completion of the first set of mouldings, here referred to as Virgin or Zero cycle, a regranulation process was carried out using a Blackfriars 2000 granulator and the subsequent material was then remoulded to produce a second set of mouldings, or the first cycle specimens. This process was repeated until the material had been remoulded from the fifth regrind.

5. Results and discussion

5.1. Infrared (I.R.) analysis

A Perkin Elmer 1600 Fourier transform infrared (FTIR) spectrophotometer was used to perform infrared analysis on the materials. Samples from each cycle under review were obtained by rubbing the relevant moulding across an abrasive disc, so obtaining particles suitable for conducting the tests. These discs were placed under an infrared beam and the resulting spectrographs were printed. Fig. 2 shows an example of the FTIR traces obtained for the virgin and the fifth recycled materials. Evidently, there are no changes in the spectra; this indicates that there is no change in the intrinsic chemical structure of the polymer under the present processing conditions.

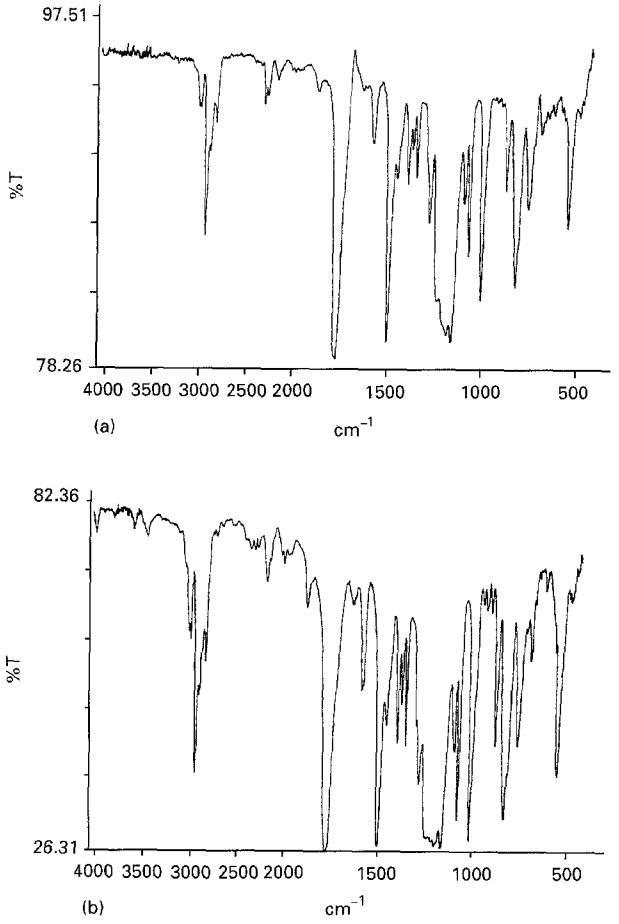

Figure 2 Infrared spectra for the (a) virgin and (b) fifth recycled materials.

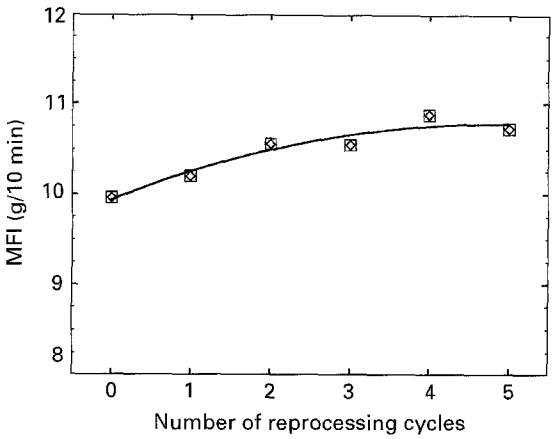

Figure 3 Melt flow index versus the number of reprocessing cycles.

5.2. Melt flow index (MFI)

The melt flow index of Makrolon 2805 was measured after each reprocessing cycle using a Davenport rheometer. Measurements were carried out as specified by ASTM D1238, at a temperature of 300 °C and with a 1.2 kg load.

After repeated recycling, the clear PC showed progressive darkening. This observation indicated that some form of degradation occurs during recycling. Fig. 3 shows the plot of MFI as a function of reprocessing cycles, where each data point represents an average value taken from at least four measurements. As can be seen, MFI increases slightly from a value of 9.98 g/10 min for the virgin material to a value of 10.73 g/10 min for the fifth recycled material. This slight increase in fluidity of the reprocessed materials is attributed to the decrease in the molecular weight of the polymer, arising from the reduction in polymeric chain lengths caused by degradation during processing as previously reported [1, 2].

5.3. Dynamic mechanical analysis (DMA)

DMA tests were conducted on a Perkin Elmer 7 series using a three-point bend configuration. Test specimens

were cut from the moulded plaques (Fig. 1) and tested at a frequency of 50 Hz, dynamic force of 80 mN and static force of 100 mN. The temperature range over which testing was conducted was between 30–200 °C with an increment of 5 °C min^{-1}.

Fig. 4 shows typical traces of storage modulus and tan δ for the virgin and few selected reprocessed materials. Results obtained from these tests indicate that there is no significant variation in the dynamic properties with the number of reprocessing cycles. Although glass transition temperature, T_g, of the reprocessed materials was similar to that of the virgin material (i.e. 155–157 °C), the range over which it occurred was broadened somewhat with the number of reprocessing cycles. This indicates a broader range of molecular weight over which the transition acts, as the material is reprocessed.

5.4. Tensile and flexural tests

Tensile and flexural tests were performed on the dumbbells and the flexural bars, respectively. All the tests were performed on an Instron testing machine at a crosshead speed of 5 mm min^{-1}. Flexural bars were tested in three-point bending with span to depth ratio of 16:1. The quantities measured from the recorded load–displacement diagrams (see Fig. 5) were: nominal tensile yield strength, σ_{yt} (calculated based on the maximum load); nominal tensile breaking strength, σ_{bt}; work to fracture, U, (determined from the area under the tensile load–displacement diagram); flexural strength, σ_{yb} (calculated based on the maximum load on the trace); and flexural modulus, E_b (calculated based on the initial slope of the load–displacement diagram).

Results obtained from these tests are summarized in Table I, where each value represents an average of five measurements. Results clearly indicate that there is no significant change in any of the quantities with the number of reprocessing cycles. Flexural strengths were consistently higher than tensile strength by a factor of 1.45. This was due to the occurrence of some degree of yielding (or plastic collapse) during the flexure tests.

Additional tests were also performed on dumbbell specimens containing a weldline. Results from these tests (see Table I) indicated that reprocessing has no significant effect upon weldline strength, σ_{yw}. The weldline integrity factor, defined as the ratio of weldline strength divided by the strength of the weld-free specimen ranged from 0.99–0.94, showing no systematic variation with the number of reprocessing cycles.

5.5. Notched impact strength tests

Notched impact strength tests were performed on the flexural bars using a Charpy impact tester. Specimens were notched to a/D ratio of 0.3, where a is the crack length and D is specimen width, using a V-shaped cutter with tip radius of 0.25 mm. Specimens were then impacted in a three-point bend configuration with span to depth ratio of 4:1 at a pendulum speed of 3 m s^{-1}. Impact energy per unit ligament area was then calculated for each specimen and plotted versus the number of reprocessing cycles as shown in Fig. 6. As can be seen, impact strength decreases with the number of reprocessing cycles. The average value for the fifth recycled material is almost 30% lower than that of the virgin material.

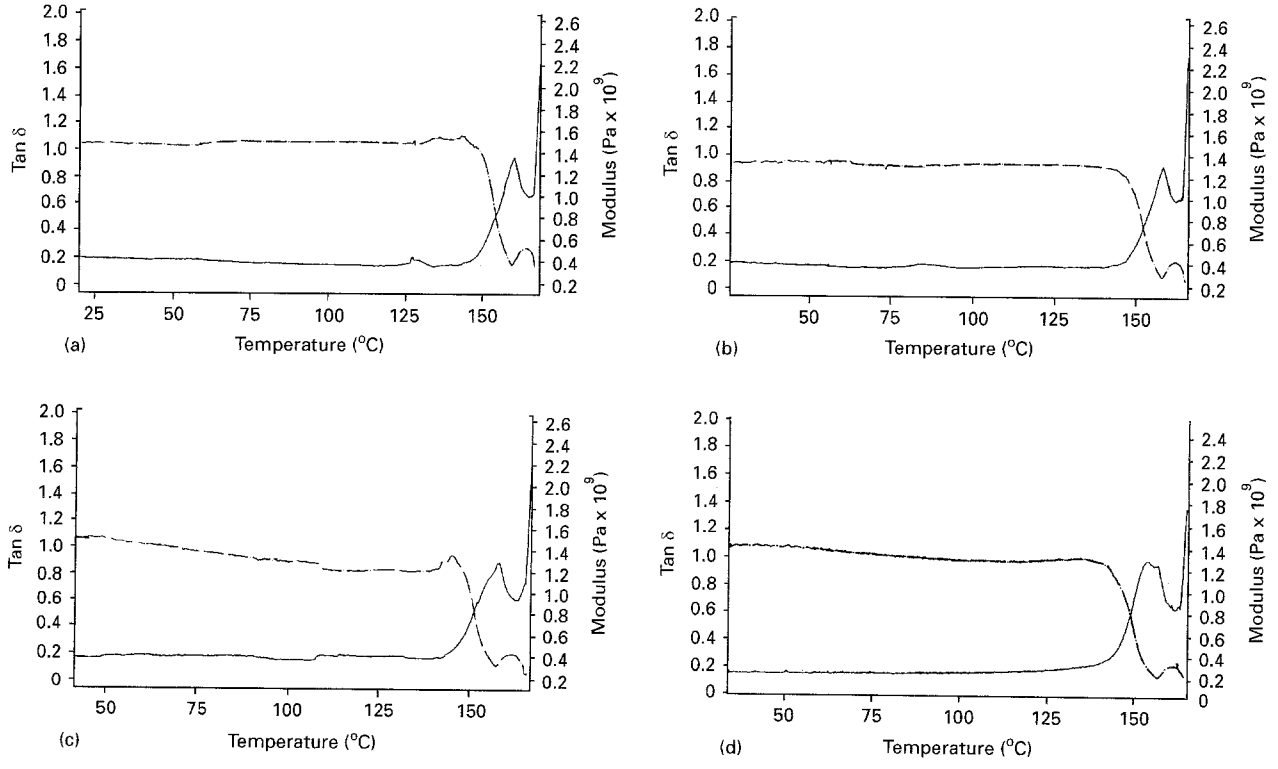

Figure 4 Typical DMA traces. (a) Virgin, (b) first cycle, (c) third cycle, (d) fifth cycle. - - - storage modulus; — loss tangent.

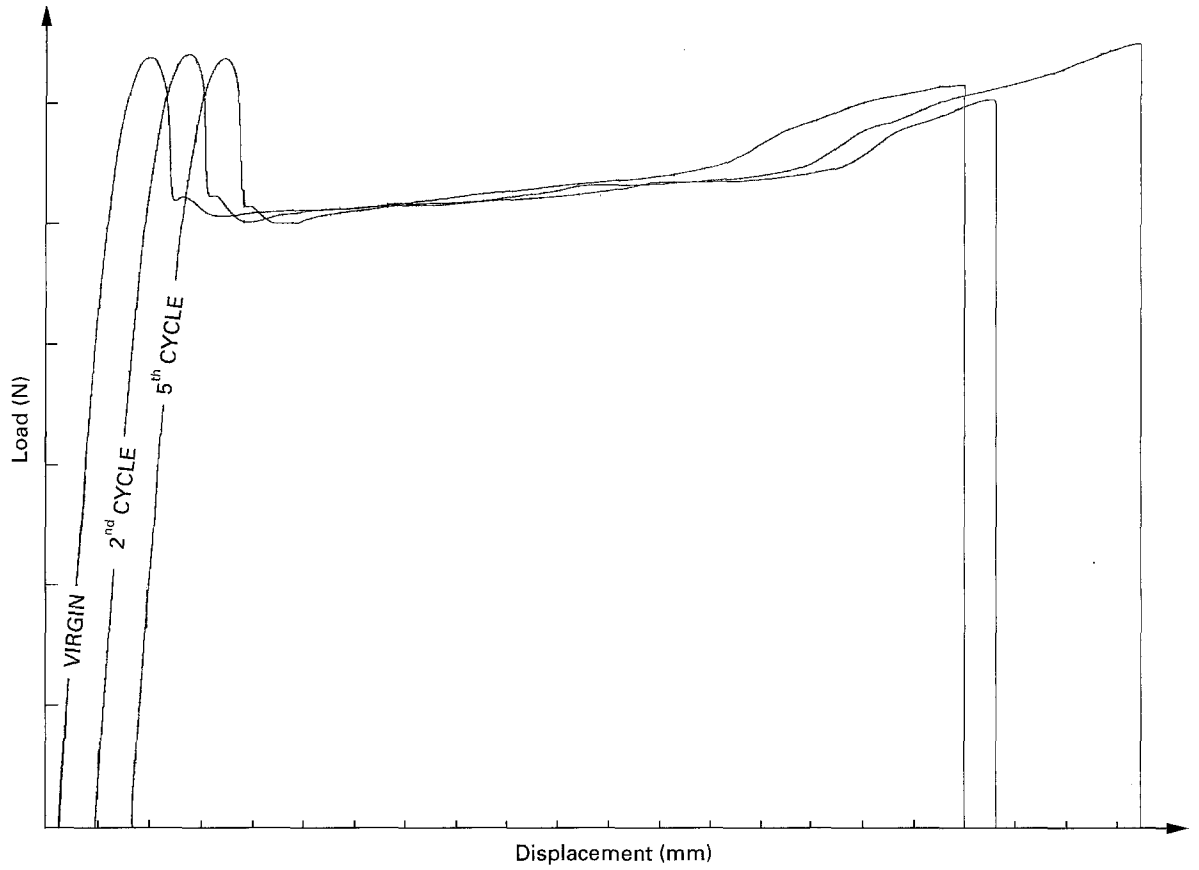

Figure 5 Typical tensile load–displacement diagrams for the virgin and the fifth recycled material.

TABLE I Tensile and flexural data

No.	σ_{yt} (MPa)	σ_{bt} (MPa)	U (J)	σ_{yw} (MPa)	σ_{yb} (MPa)	E_b (GPa)
0	61.22	59.12	54.70	59.79	88.26	1.81
1	60.59	58.72	51.59	60.03	88.26	1.86
2	63.09	62.14	63.80	59.01	88.38	1.85
3	60.22	58.99	52.76	58.55	88.51	1.88
4	60.42	59.55	54.22	59.94	88.64	1.86
5	60.27	55.90	55.50	59.41	88.26	1.88

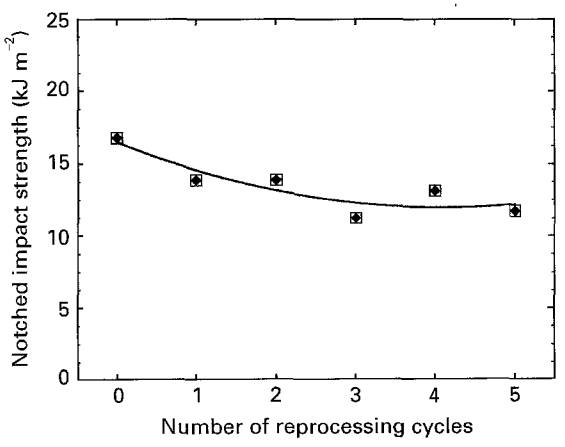

Figure 6 Notched impact strength versus the number of reprocessing cycles.

5.6. Tensile testing of notched bars

5.6.1. Fracture toughness

Fracture testing of notched bars was performed on single-edge notched tension (SENT) specimens (see Fig. 7). Rectangular coupons of nominal dimensions

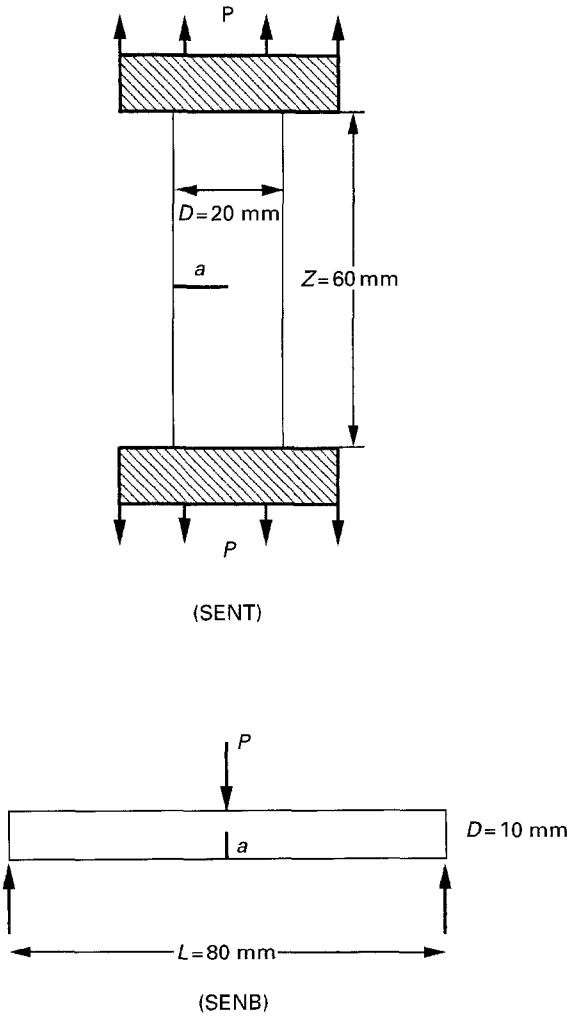

Figure 7 SENT and SENB fracture specimens.

$1.7 \times 20 \times 88$ mm were cut from the plaque mouldings and then edge notched to various a/D ratios ranging from 0.1–0.7 using a razor blade. These SENT specimens were then tested to complete failure in an Instron testing machine at a constant crosshead speed of $2\,\text{mm}\,\text{min}^{-1}$ using pneumatic clamps with a gauge length of 60 mm. The load–displacement trace for each specimen was recorded for the subsequent analysis.

The nature of the SENT load–displacement diagram for the virgin and the reprocessed materials is typified by the traces shown in Fig. 8. They show that the nature of failure is by slow crack growth from the notch tip. The plot of the maximum stress σ_{max} versus a/D for the virgin and the reprocessed materials is shown in Fig. 9, where it can be seen that maximum stress is not affected by the number of reprocessing cycles. Using the linear elastic fracture mechanics (LEFM) relationship

$$\sigma_{max} = \frac{K_{max}}{Ya^{1/2}} \tag{1}$$

the value of fracture toughness at maximum load K_{max} was calculated from the slope of the line σ_{max} versus $1/Ya^{1/2}$. The finite width geometrical function Y is expressed in terms of a/D ratio as [4]

$$Y = \frac{5\pi^{1/2}}{[20 - 13(a/D) - 7(a/D)^2]^{1/2}} \tag{2}$$

Fig. 10 shows σ_{max} versus $1/Ya^{1/2}$ for the virgin and the reprocessed materials. Evidently, for a certain range of a/D ratio, variation is extremely linear and therefore independent of the crack length as required by LEFM. K_{max} values calculated for each specimen are shown in Fig. 11. Clearly, there is a pronounced R-curve effect for a/D ratios less than 0.2, where K_{max} increases as a/D ratio increases. The slope of the line in Fig. 10, or alternatively the plateau value in Fig. 11 indicate that K_{max} is indeed independent of the number of reprocessing cycles and for the specimen dimensions used here attains a constant value of 5.2 MPa $m^{1/2}$. It should be first pointed out that, technically speaking, the results are satisfactory and do not depend on the length of the crack when a/D ratio exceeds 0.2; only the size of the specimen may modify the results. The effect of the specimen size on K_{max} was investigated using SENT specimens with varying widths, D, ranging from 5 mm to 40 mm. Fig. 12(a) shows the variation of σ_{max} with crack length for these specimens. Clearly, the effect of increasing specimen width is to shift the σ_{max} versus a plot horizontally to the right. However, if these σ_{max} values are plotted as

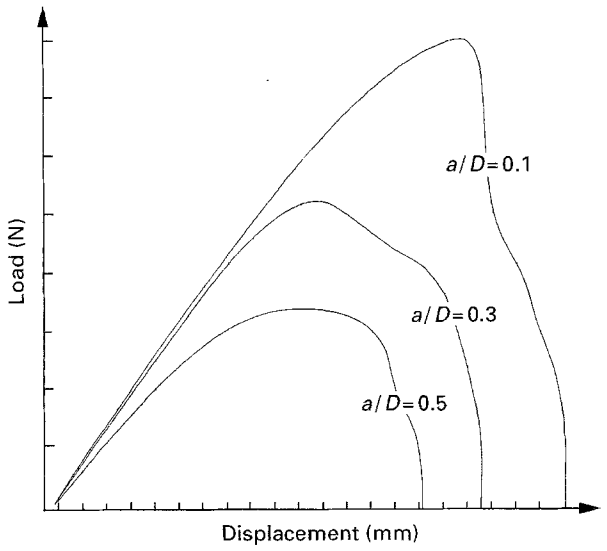

Figure 8 Typical SENT specimens for various crack lengths.

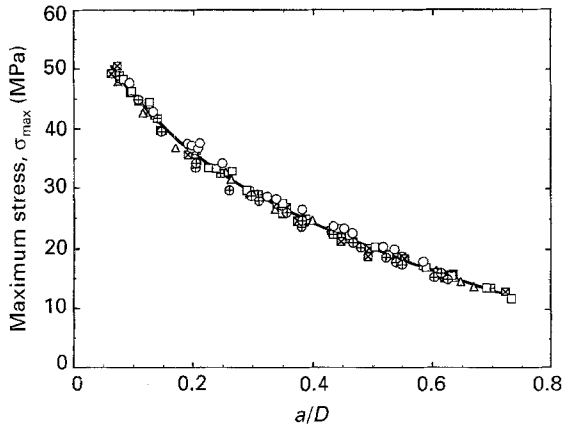

Figure 9 Maximum stress versus a/D ratio for the virgin and the reprocessed materials using SENT specimens. ○ 0; ⊕ 1st; □ 2nd; ⊞ 3rd; ⊠ 4th; △ 5th.

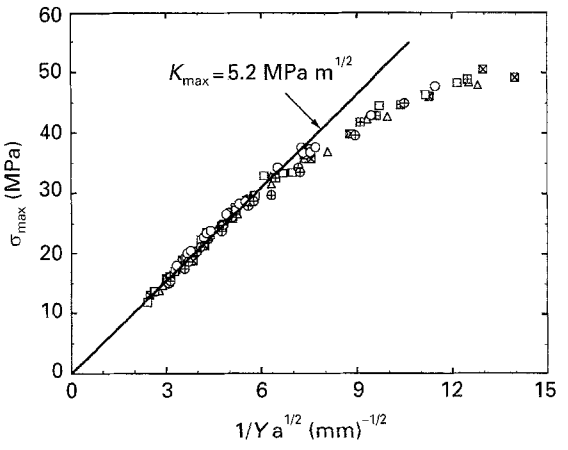

Figure 10 Maximum stress versus $1/Ya^{1/2}$ for the virgin and the reprocessed materials using SENT specimens. ○ 0; ⊕ 1st; □ 2nd; ⊞ 3rd; ⊠ 4th; △ 5th.

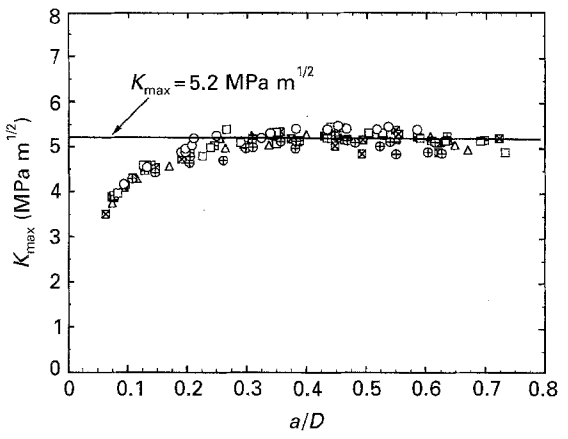

Figure 11 Fracture toughness at maximum stress K_{max} versus a/D for SENT specimens. ○ 0; ⊕ 1st; □ 2nd; ⊞ 3rd; ⊠ 4th; △ 5th.

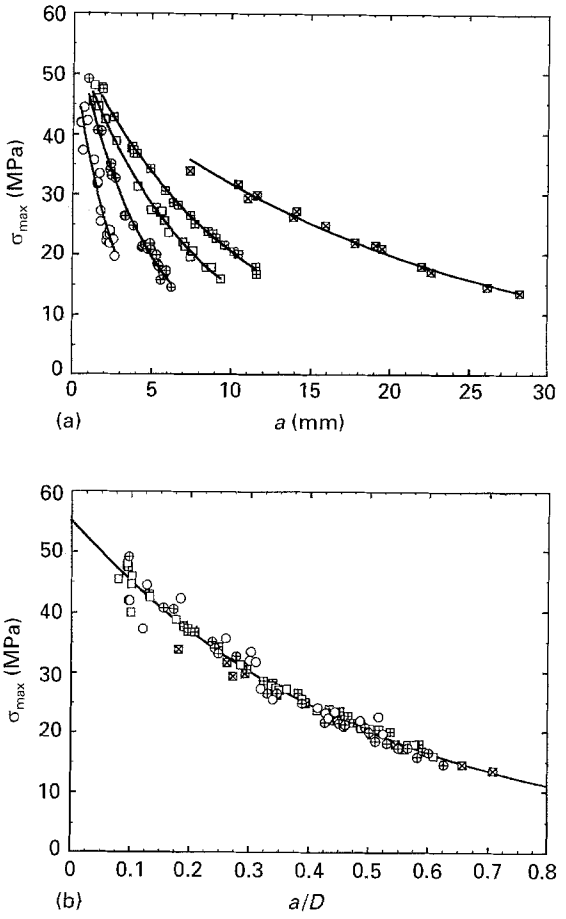

Figure 12 (a) Maximum stress versus crack length for various specimen widths using SENT specimens. (b) Maximum stress a/D ratio for various specimen widths using SENT specimens. ○ 5 mm; ⊕ 10 mm; □ 15 mm; ⊞ 20 mm; ⊠ 40 mm.

a function of a/D ratio as illustrated in Fig. 12(b), then one may observe that for a given a/D ratio, σ_{max} becomes more or less independent of sample width. Using Equation 1, K_{max} for each specimen was calculated and plotted against a/D ratio as shown in Fig. 13. The results show that for each sample width, K_{max} initially rises with a/D (R-curve effect) before reaching a plateau where its value becomes more or less independent of a/D ratio; the plateau value increases with sample width. To explain this increase in K_{max} with specimen width, Equation 1 was written in the following form

$$K_{max} = D^{1/2}\left(\frac{a}{D}\right)^{1/2} Y\left(\frac{a}{D}\right)\sigma_{max} \quad (3)$$

Considering that for a given a/D ratio, the product term $(a/D)^{1/2}Y(a/D)\sigma_{max}$ is independent of D, then according to Equation 3 K_{max} should increase with specimen width according to

$$K_{max} = CD^{1/2} \quad (4)$$

where C is a constant. The experimental results shown in Fig. 14 illustrate that, for the range of sample widths tested here, K_{max} is indeed proportional to the square root of sample width, D. The constant C is 1.13 MPa mm$^{-1/2}$ where K_{max} has units of MPa m^{-1} and D is in mm, or 32.75 MPa when D has units of m. (Note that there is also small positive intercept of 0.17 at $D = 0$).

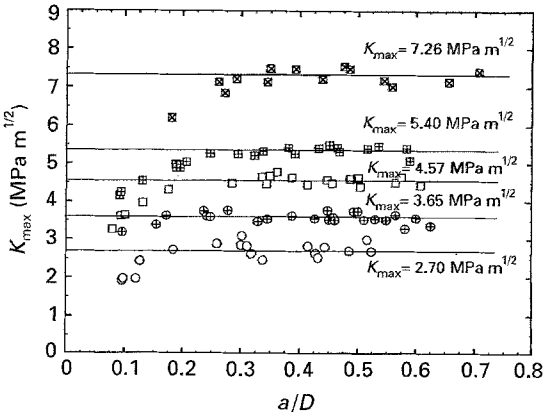

Figure 13 Fracture toughness at maximum stress versus a/D ratio for various specimen widths using SENT specimens (virgin material). ○ 5 mm; ⊕ 10 mm; □ 15 mm; ⊞ 20 mm; ⊠ 40 mm.

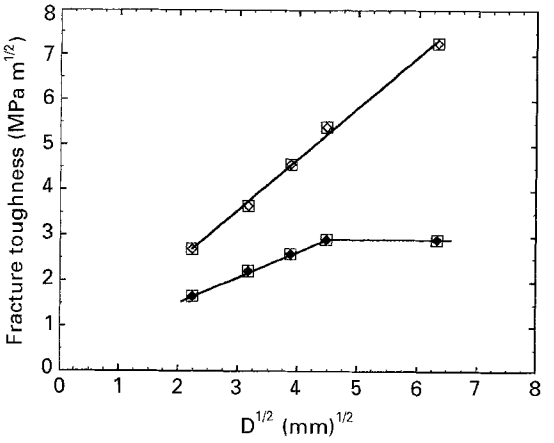

Figure 14 Fracture toughness at maximum stress (⊠) and at initiation(●) versus square root of sample width $D^{1/2}$ for SENT specimens.

Fig. 15 shows a series of photographs taken from several specimens of varying crack lengths. These photographs show the evolution of a damage zone in the form of a craze at the tip of the crack which led to slow crack growth that was noted in all the specimens. To measure the length of this zone, ρ, at maximum load, a minimum of ten specimens for each width of varying crack lengths were loaded up to the maximum load and then unloaded. After unloading, zone length was measured for each specimen with the aid of an optical microscope. Measurements indicated that, whereas for a given sample width, zone length ρ is not affected by the length of the initial crack, its value increased with increasing sample width in the manner shown in Fig. 16(a) where

$$\rho = 2.12D^{1/2} - 3.504 \quad (5)$$

Moreover variation of K_{max} with zone length, ρ, was also linear, as shown in Fig. 16(b) where

$$K_{max} = 0.53\,\rho + 2.08 \quad (6)$$

(K_{max} has units of MPa m$^{1/2}$ and ρ has units of mm). Substitution of Equation 6 into Equation 7 gave a relationship between K_{max} and the sample width D as

$$K_{max} = 1.12D^{1/2} + 0.23 \quad (7)$$

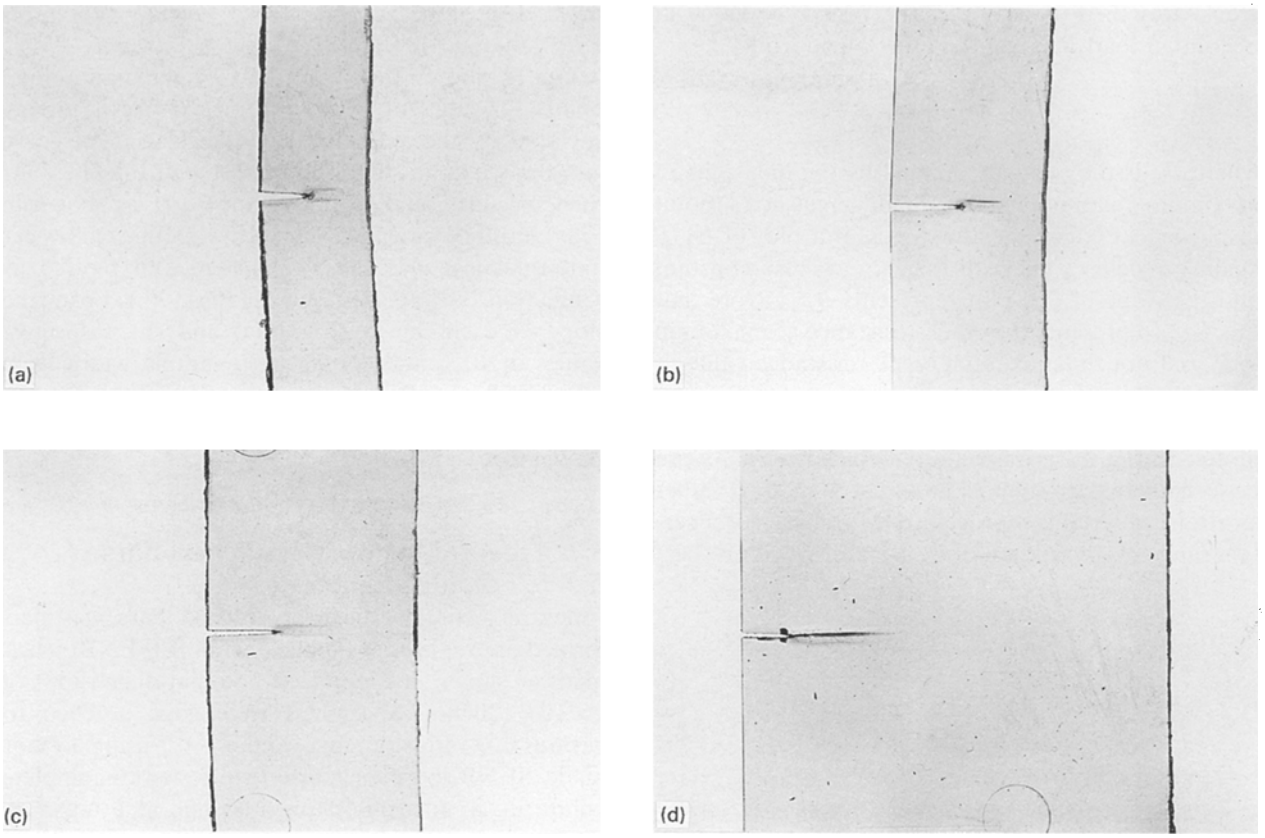

Figure 15 Typical SENT fractured specimens showing the damage zone at the crack tip at maximum load. (a) $D = 10$ mm; (b) $D = 15$ mm; (c) $D = 20$ mm; (d) $D = 40$ mm.

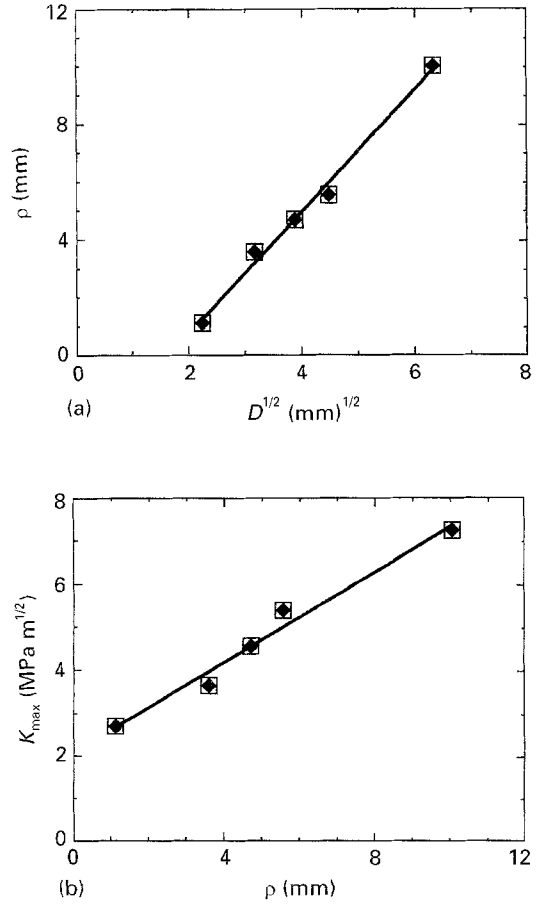

Figure 16 (a) Damage zone length ρ versus logarithm of sample width. (b) Logarithm of K_{max} versus the damage zone length.

(where D has units of mm). This equation agrees extremely well with Equation 4 thus suggesting that the increase in K_{max} with sample width stems from the increase in zone length with increasing sample width.

Finally, the onset of crack growth (i.e. initiation) was also detected visually to determine the value of the fracture toughness at initiation K_{init}. These values are also plotted in Fig. 14 as a function of $D^{1/2}$. Evidently for sample widths less than 20 mm, K_{init} increases linearly with $D^{1/2}$, but reaches a constant value of 2.92 MPa m$^{1/2}$ at larger widths.

5.6.2. Crack growth resistance

Crack growth resistance values for the virgin and the reprocessed materials were obtained using the generalized locus method that has been developed by Kim and Joe [5]. According to this method, the resistance to steady crack propagation R_p can be determined from the following equation

$$R_p = -\frac{1}{B}\frac{\Delta U_f}{\Delta a} \tag{8}$$

where B is the specimen thickness, a is the initial crack length, and U_f (the energy required for crack propagation) is the total area enclosed by the loading curve and the x-axis. If R_p is constant for a given specimen thickness, then a plot of U_f/B against a should yield a linear fit. The slope of this linear fit represents R_p.

Similarly, Equation 8 can be used to find the resistance value at a certain characteristic point during the

crack growth. For example, the resistance value at maximum load R_{max} can be ascertained from

$$R_{max} = -\frac{1}{B}\frac{\Delta U_L}{\Delta a} \quad (9)$$

where U_L is the area surrounded by the locus line of maximum load points, the load versus load point displacement curve and the x-axis. If a plot of U_L/B against a yields a linear fit then R_{max} is also constant and the slope of this plot represents R_{max}. Note that this R_{max} represents the crack resistance at maximum load and not the maximum crack resistance value.

The total energy per unit thickness for fracture (U_f/B) of each virgin and reprocessed specimen is plotted in Fig. 17 as a function of crack length. As can be seen, there is no significant variation in U_f/B values as virgin material is reprocessed. Moreover, for a certain range of a, variation of U_f/B is linear with respect to a. The slope of this linear portion represents a R_p value of 148 kJ m^{-2}.

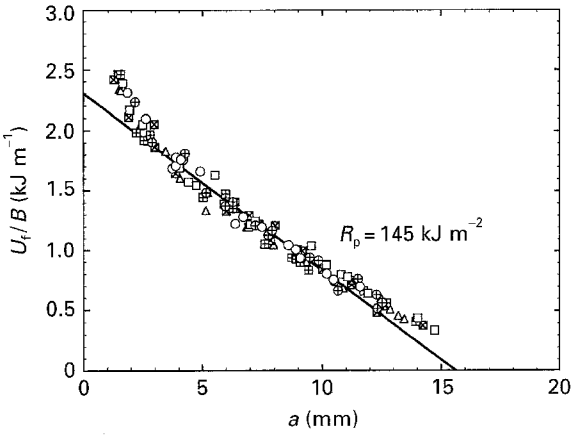

Figure 17 U_f/B versus crack length for the virgin and the reprocessed material using SENT specimens. ○ 0; ⊕ 1st; □ 2nd; ⊞ 3rd; ⊠ 4th; △ 5th.

Fig. 18 shows the locus line of maximum load points for different widths. For each width, energy enclosed by the locus line, load–displacement curve and the x-axis was determined per unit thickness for each specimen, and plotted against a/D, as shown in Fig. 19(a). The total areas under the loading curves per unit thickness were also calculated and plotted as a function of a/D, as shown in Fig. 19(b). From the slope of each line in Fig. 19(a) and (b), respective values of R_{max} and R_p for each sample width were calculated ($= 1/D \times$ slope). It was found that these values were also fairly linear with respect to $D^{1/2}$ as shown in Fig. 19(c).

5.7. Flexural testing of notched bars

5.7.1. Fracture toughness

Fracture testing of flexural notched bars was performed on single-edge notched bending (SENB) specimens as shown in Fig. 7 with nominal dimensions of $4 \times 10 \times 120$ mm. Specimens were edge notched to various a/D ratios ranging from 0.1–0.7 using a razor blade. SENB specimens were then tested to complete failure in an Instron testing machine at a constant crosshead speed of 5 mm min^{-1} in a three-point bend configuration with span to depth ratio of 8 : 1 (i.e. span width of 80 mm).

Fig. 20 shows typical SENB load–displacement diagrams that were obtained for most of the virgin and some of the reprocessed materials. It was noted that while failure of the virgin specimens was predominantly by ductile tearing, that of reprocessed specimens was either semi-brittle or ductile. Generally, the majority of the reprocessed specimens with a/D ratios greater than 0.3 failed unstably at close proximity to

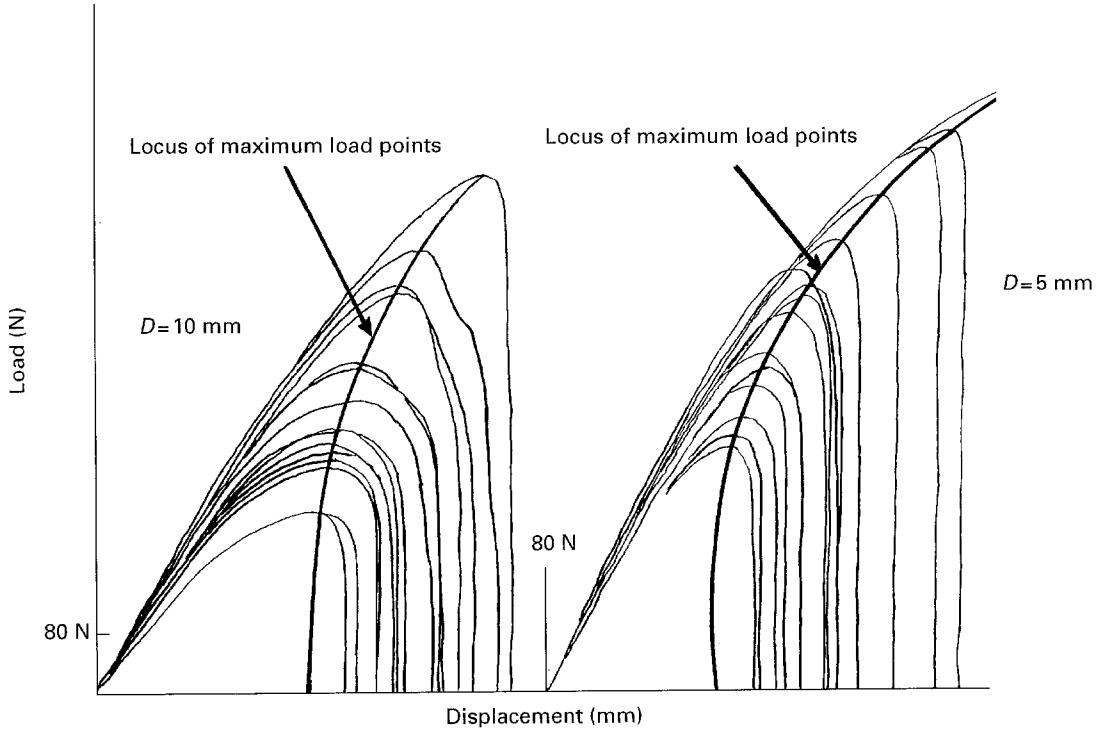

Figure 18 Typical SENT load–displacement diagrams for various widths and crack lengths showing the locus line of maximum load points.

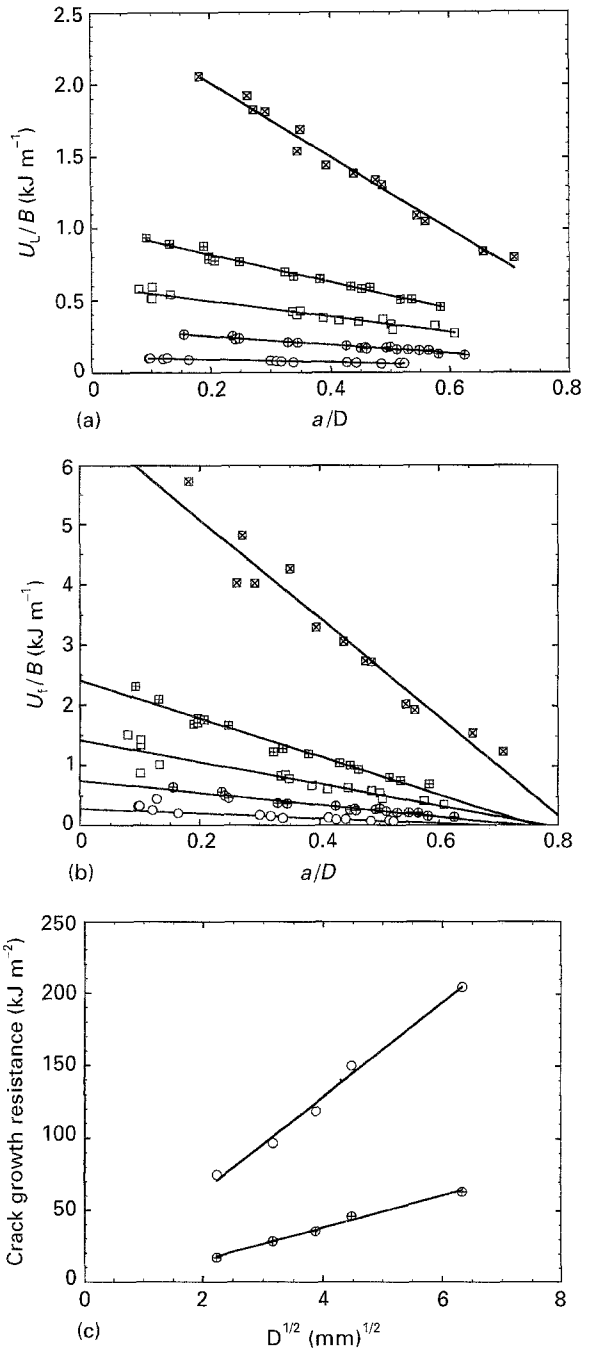

Figure 19 (a) U_f/B versus a/D for various specimen widths using SENT specimens. (b) U_L/B versus a/D for various specimen widths using SENT specimens. ○ 5 mm; ⊕ 10 mm; □ 15 mm; ⊞ 20 mm; ⊠ 40 mm. (c) R_p (○) and R_{max} (⊕) values versus $D^{1/2}$.

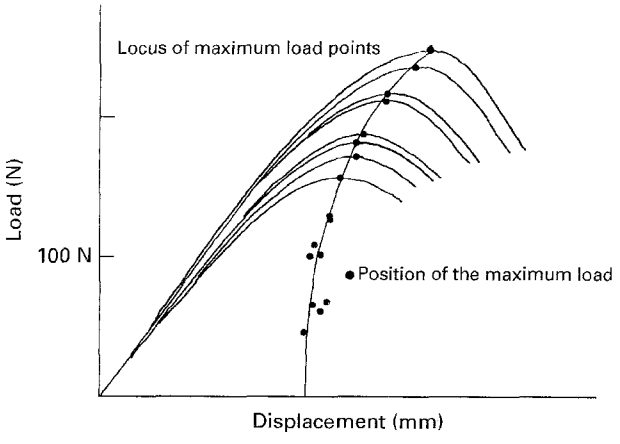

Figure 20 Load–displacement diagrams for SENB specimens.

the maximum load. The plot of the maximum stress σ_{max} versus a/D ratio was similar to that obtained for SENT specimens, as shown in Fig. 21, thus further suggesting that σ_{max} is not affected by the number of reprocessing cycles. Variation of σ_{max} with respect to $1/Y\,a^{1/2}$ (the Y function as given in ref [6]) for the virgin and the reprocessed specimens is shown in Fig. 22, and as can be seen it is effectively linear with some deviation occurring at crack length values smaller than 0.2 (R-curve effect). The best line fitted through the data gives a K_{max} value of 5.05 MPa m$^{1/2}$.

5.7.2. Crack growth resistance

Values of total work of fracture per unit thickness (U_f/B) versus crack length for specimens fracturing by ductile tearing is shown in Fig. 23. It is evident from the figure that the variation is linear for wide range of crack lengths giving a R_p value of 95 kJ m^{-2} which is independent of the number of reprocessing cycles. This value agrees quite well with the value of 97 kJ m^{-2} obtained via SENT specimens for the same sample width. The work of fracture per unit thickness, enclosed by the locus line of maximum load points (see Fig. 18), load–displacement diagram and the x-axis was calculated for each virgin and the fifth recycled

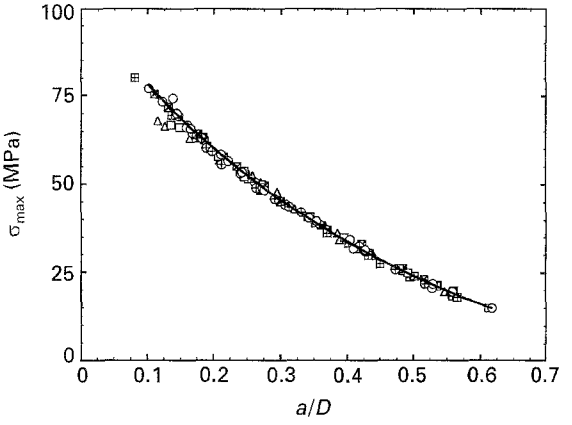

Figure 21 Maximum stress versus a/D ratio for the virgin and the reprocessed materials using SENB specimens. ○ 0; ⊕ 1st; □ 2nd; ⊞ 3rd; ⊠ 4th; △ 5th.

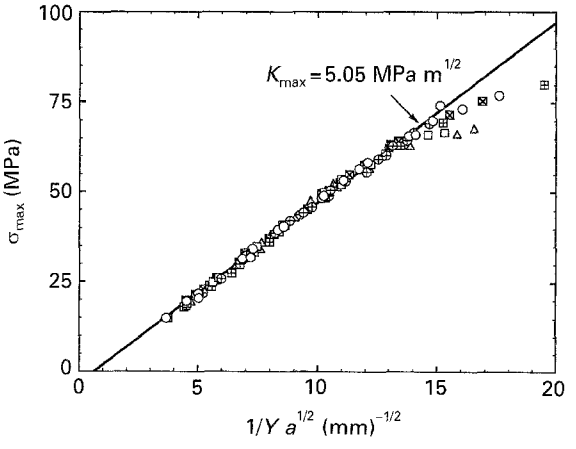

Figure 22 Maximum stress versus $1/Y\,a^{1/2}$ for the virgin and the reprocessed materials using SENB specimens. ○ 0; ⊕ 1st; □ 2nd; ⊞ 3rd; ⊠ 4th; △ 5th.

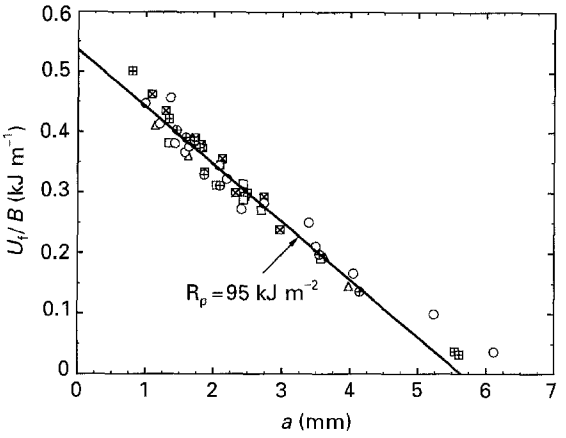

Figure 23 U_f/B for ductile failures versus crack length for the virgin and the reprocessed materials using SENB specimens. ○ 0; ⊕ 1st; □ 2nd; ⊞ 3rd; ⊠ 4th; △ 5th.

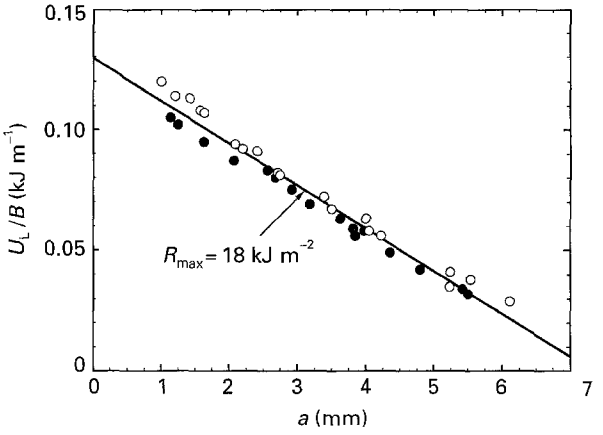

Figure 24 U_L/B versus crack length for the virgin (○) and the fifth (●) recycled materials.

specimens. Values of U_L/B are plotted in Fig. 24 as a function of crack length. As can be seen the relationship between U_L/B and crack length is quite linear giving a R_{max} value of 18 kJm^{-2}, which is more or less independent of the number of reprocessing cycles. This value of R_{max} is 40% lower than that obtained via SENT specimens for the same specimen width. This indicates that whereas the value of R_p for a given specimen width is independent of the specimen geometry, the value of R_{max} is geometry dependent.

6. Summary

The influence of reprocessing by injection moulding on properties of polycarbonate has been studied. It is found that:

1. The infrared spectrum is not affected by the number of reprocessing cycles. This indicates that the chemical structure of the polymer remains unaffected by reprocessing.
2. The melt flow index (MFI) increases slightly with the number of reprocessing cycles due to increase in molecular weight with the number of reprocessing cycles.
3. The dynamic mechanical properties (storage modulus and loss tangent) are not significantly affected by the number of reprocessing cycles. The glass transition temperature was also not affected by reprocessing; however, the range over which it occurred was broadened somewhat by reprocessing due to increase in molecular weight with the number of reprocessing cycles.
4. Reprocessing does not affect the basic mechanical properties such as tensile strength, flexural strength and flexural modulus.
5. The notched impact strength, showed some variation with the number of reprocessing cycles.
6. Fracture stresses obtained by way of SENT and SENB specimens showed no significant variation with the number of reprocessing cycles.
7. Fracture toughness was not affected by the number of reprocessing cycles.
8. Resistance to steady state crack propagation R_p was not affected by the number of reprocessing cycles.

Acknowledgements

The authors gratefully acknowledge the support of Bayer UK for providing the material.

References

1. K. B. ABBAS, *Polym. Eng. Sci.* **20** (1980) 376.
2. J. I. EGUIAZABAL and J. NAZABAL, *Eur. Polymer* **14** (1989) 891.
3. A. CHRYSOSTOMOU and S. HASHEMI, *J. Mater. Sci.* **31** (1996) 1183.
4. D. O. HARRIS, *J. Bas. Eng.* **49** (1967) 89.
5. B. H. KIM and C. R. JOE, *Eng. Fract. Mech.* **34** (1989) 221.
6. W. F. BROWN and J. E. SRAWLEY, ASTM STP 410 (1966).

Received 8 December 1995
and accepted 15 January 1996